




Two 5-tetrazolylazo-8-hydroxyquinoline-based Zn(II) and Mn(II) complexes: syntheses, structures and optical properties

Yan-Xuan Qiu, Wen-Ning Lin, Zhi-Xin Li, Zhi-Jian Ou Yang, Liu Yang & Wen Dong


To cite this article: Yan-Xuan Qiu, Wen-Ning Lin, Zhi-Xin Li, Zhi-Jian Ou Yang, Liu Yang & Wen Dong (2015) Two 5-tetrazolylazo-8-hydroxyquinoline-based Zn(II) and Mn(II) complexes: syntheses, structures and optical properties, Journal of Coordination Chemistry, 68:22, 3945-3953, DOI: [10.1080/00958972.2015.1080824](https://doi.org/10.1080/00958972.2015.1080824)

To link to this article: <http://dx.doi.org/10.1080/00958972.2015.1080824>

 View supplementary material 

 Accepted author version posted online: 13 Aug 2015.
Published online: 28 Aug 2015.

 Submit your article to this journal 

 Article views: 143

 View related articles 

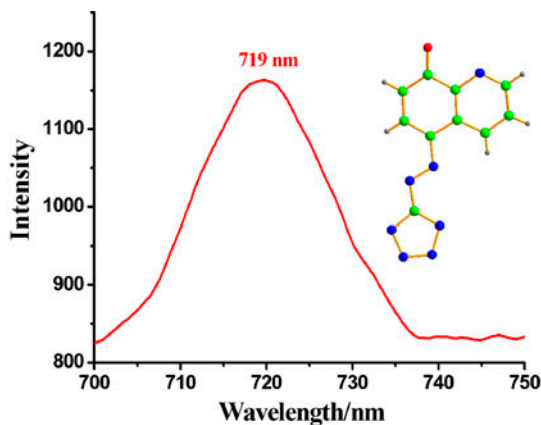
 View Crossmark data 

Two 5-tetrazolylazo-8-hydroxyquinoline-based Zn(II) and Mn(II) complexes: syntheses, structures and optical properties

YAN-XUAN QIU, WEN-NING LIN, ZHI-XIN LI, ZHI-JIAN OU YANG, LIU YANG and WEN DONG*

Department of Chemistry, Guangzhou Key Laboratory for Environmentally Functional Materials and Technology, Guangzhou University, Guangzhou, PR China

(Received 30 January 2015; accepted 10 July 2015)



Two 5-tetrazolylazo-8-hydroxyquinoline (TTHQ) Zn²⁺ and Mn²⁺ complexes, [Zn(TTHQ)(en)]·2H₂O (en = ethylenediamine) (**1**) and [Mn₂(TTHQ)₂(H₂O)₆]·2H₂O (**2**), were synthesized and characterized by single-crystal X-ray diffraction analysis. Stacking (π - π) and hydrogen-bonding interactions are responsible for the stabilization of the supramolecular structures. UV-vis spectral changes and photoluminescent properties of TTHQ, **1** and **2** were investigated and a red emission was found. The hydrogen-bonding interaction energies in **1** and **2** were calculated using density functional theory at the WB97XD/6-31++G level.

Keywords: 8-Hydroxyquinoline derivatives; Crystal structure; Red photoluminescence; DFT

1. Introduction

Since a tris-8-hydroxyquinoline (HQ) Al³⁺ complex, AlQ₃, was successfully used as a luminescent material [1], HQ and numerous derivatives, as well as metal complexes, have attracted attention of researchers for a wide range of applications (e.g. organic light emitting

*Corresponding author. Email: dw320@aliyun.com

diodes (OLED), optoelectronic devices [1–4], imaging with radionuclides [5], pharmaceuticals, drugs in cancer treatment such as tumor growth inhibitors [6, 7] and neurodegenerative disorders [8]). Zinc complexes with 8-hydroxyquinoline, which is the most widely used electron-transporting material in OLEDs, may enhance electron-transporting for OLEDs [9, 10]. However, HQ itself is only weakly fluorescent owing to the excited-state intramolecular proton transfer process from oxygen to nitrogen; its numerous derivatives show only yellowish-green emission [11–13]. Modification of HQ by changing substituents at 2-, 5-, or 7-positions can change solubility, emission wavelength, luminescent intensity, and HOMO and LUMO energy levels [11, 14–17]. The highest HOMO electron density of HQ is on the 5-position and corresponding electron-withdrawing and/or -donating substituents affect properties of the resulting complexes [18, 19]. Among HQ derivatives, azo conjugated 8-hydroxyquinoline derivatives and complexes have been reported because the azo group ($-\text{N}=\text{N}-$) usually undergoes reversible *trans-cis* photoisomerization that can be exploited in the design of photoswitches, molecular motors, memory storage devices, etc. [20–26]. Inspired by these literature reports, we tried to manipulate the HOMO–LUMO energy gap to achieve the requirement for red emission via attaching photochromic scaffolds of tetrazolylazo to 5-position of the HQ skeletal. Here, the 5-substituted-8-hydroxyquinoline derivative of TTHQ was synthesized and crystal structures of **1** and **2**, and optical properties, are reported.

2. Experimental

2.1. Materials and instrumentations

All commercial reagents and solvents were used without purification unless otherwise stated. ^1H NMR spectra were recorded on a 400 MHz Digital NMR Spectrometer. IR spectra were recorded as pressed KBr pellets on a Bruker Tensor 27 spectrophotometer with an average of 64 scans. Elemental analyses were carried out using a Perkin-Elmer analyzer model 240. UV–vis absorption spectra were recorded with a U-2250 UV Spectrophotometer. The excitation spectrum and emission spectra were recorded on an F-4500 Fluorescence Spectrophotometer. Photoluminescence quantum yield (QY) was calculated using an integrating sphere within the FLSP920 (Edinburgh Instruments) by an absolute method.

2.2. Syntheses of TTHQ, **1** and **2**

2.2.1. Synthesis of TTHQ. The preparation of TTHQ can be readily achieved by a two-step reaction (Supplementary Material, scheme S1). Yield of TTHQ: 72%. IR (KBr, cm^{-1}): 3416s, 3068m, 1627m, 1547m, 1379m, 1229w, 1049m, 832m, 751m. Elemental analysis: Anal. Calcd for TTHQ (%) $\text{C}_{10}\text{H}_7\text{N}_7\text{O}$, Mr = 241: C, 49.79; H, 2.90; N, 40.66. Found (%): C, 49.66; H, 2.74; N, 40.48. ^1H NMR (400 MHz, DMSO) δ = 9.43 (d, J = 6.7 Hz, 1H), 9.03 (s, 1H), 8.25 (d, J = 8.9 Hz, 1H), 7.89 (dd, J = 8.5, 4.2 Hz, 1H), 7.26 (s, 1H) (Supplementary Material, figure S1). MS (ESI) for TTHQ m/z $[\text{M} - \text{H}]^-$ $\text{C}_{10}\text{H}_6\text{N}_7\text{O}^-$ requires: 240.0, found: 239.9; $[\text{M} + \text{H}]^+$ $\text{C}_{10}\text{H}_8\text{N}_7\text{O}^+$ requires: 242.0, found: 242.0.

2.2.2. Synthesis of $[\text{Zn}(\text{TTHQ})(\text{en})]\cdot 2\text{H}_2\text{O}$ (1**).** A mixture of $\text{Zn}(\text{NO}_3)_2\cdot 6\text{H}_2\text{O}$ (59.4 mg, 0.2 mmol) and 5-tetrazolylazo-8-hydroxyquinoline (24.2 mg, 0.1 mmol) in 10 mL of water and 10 mL of ethanol was stirred for 5 min and a red precipitate formed. To the above

mixture, 18.0 mg (0.3 mmol) of ethylenediamine in 5 mL of water was added. The red precipitates slowly dissolved giving a dark red solution. The dark red solution was heated and stirred for 6 h, filtered, and dark red crystals were obtained by slow evaporation of the filtrate for several days. The dark red crystals were washed with 95% ethanol, yield: 67% (based on Zn^{2+}). IR (KBr, cm^{-1}): 3635s, 3426m, 3297m, 1567m, 1507m, 1329m, 1248m, 1041m, 832s, 662s. Elemental analysis: Anal. Calcd for **1** (%) $\text{C}_{12}\text{H}_{17}\text{N}_9\text{O}_3\text{Zn}$, $M_r = 400.74$: C, 35.98; H, 4.28; N, 31.46. Found (%): C, 35.71; H, 4.60; N, 31.61.

2.2.3. Synthesis of $[\text{Mn}_2(\text{TTHQ})_2(\text{H}_2\text{O})_6] \cdot 2\text{H}_2\text{O}$ (2**).** $\text{NH}_3 \cdot \text{H}_2\text{O}$ (18%) was added to a solution of 5-tetrazolylazo-8-hydroxyquinoline (48.4 mg, 0.2 mmol) in 10 mL of ethanol to adjust pH to 6. Then, $\text{MnCl}_2 \cdot 4\text{H}_2\text{O}$ (39.6 mg, 0.2 mmol) in 10 mL of water was added slowly to the above solution and stirred for 1.5 h. The resulting mixture was filtered and block red crystals of **2** were obtained by slow evaporation of the filtrate after several days and washed with 95% ethanol, yield: 58% (based on Mn^{2+}). IR (KBr, cm^{-1}): 3079m, 1573m, 1505m, 1469m, 1395m, 1328s, 1249s, 1205m, 1101m, 791w, 719w. Elemental analysis: Anal. Calcd for **2** (%) $\text{C}_{20}\text{H}_{30}\text{Mn}_2\text{N}_{14}\text{O}_{12}$, $M_r = 768.46$: C, 31.23; H, 3.90; N, 25.51. Found (%): C, 31.08; H, 3.79; N, 25.44.

2.3. X-ray crystallography and data collection

The crystals were filtered from the solution and immediately coated with hydrocarbon oil on the microscope slide. Suitable crystal was mounted on a glass fiber with silicone grease and placed in a Bruker Smart APEX(II) area detector using graphite-monochromated Mo-K α radiation ($\lambda = 0.71073 \text{ \AA}$) at 296(2) K. The crystallographic structures were solved by direct methods and successive Fourier difference syntheses (SHELXS-97) and refined by full-matrix least squares on F^2 with anisotropic thermal parameters for all non-hydrogen atoms (SHELXL-97) [27, 28]. Hydrogens were added theoretically and were allowed to ride on the parent atoms. Crystallographic data were deposited in the Cambridge

Table 1. The crystal data and collection parameters for **1** and **2**.

Parameters	1	2
Formula	$\text{C}_{12}\text{H}_{17}\text{N}_9\text{O}_3\text{Zn}$	$\text{C}_{20}\text{H}_{30}\text{Mn}_2\text{N}_{14}\text{O}_{12}$
M_r	400.74	768.46
Crystal system	Monoclinic	Monoclinic
Space group	$P2_1/c$	$P2_1/c$
a (\AA)	14.1934(5)	7.7465(5)
b (\AA)	9.1356(3)	7.9386(5)
c (\AA)	12.4572(4)	25.0488(18)
α ($^\circ$)	90	90
β ($^\circ$)	97.376(2)	91.182(4)
γ ($^\circ$)	90	90
V (\AA^3)	1601.90(9)	1540.08(18)
Z	4	2
ρ_{calc} (g cm^{-3})	1.662	1.657
μ (mm^{-1})	1.569	0.903
$F(0\ 0\ 0)$	824.0	788.0
R_1^a	0.0386	0.0312
wR_2^b	0.0952	0.0729

$$^a R = \sum \|F_o - |F_c| \| / \sum |F_o|; \quad ^b wR_2 = \left[\sum w(F_o^2 - F_c^2)^2 / \sum w(F_o^2) \right]^{1/2}.$$

Crystallographic Database Center: CCDC-975072 for **1** and 1036107 for **2**. The crystal data and collection parameters for **1** and **2** are listed in table 1.

2.4. Quantum calculations

All quantum-chemical calculations were carried out by the Gaussian 09 suite [29]. The calculations of hydrogen-bonding interaction energies were carried out using density functional theory (DFT) with the WB97XD procedure and MP2 at 6-31++G level based on the crystal structures obtained in this work. The interaction energies were counterpoise corrected with the procedure of Boys and Bernardi in order to account for the basic set superposition error [30].

3. Results and discussion

3.1. Crystal structures

3.1.1. The crystal structure of $[\text{Zn}(\text{TTHQ})(\text{en})]\cdot 2\text{H}_2\text{O}$ (1**).** The atomic labeling diagram of **1** is shown in figure 1(a). Complex **1** crystallizes in the monoclinic space group $P2_1/c$. Each asymmetric unit of **1** consists of one Zn^{2+} , one TTHQ^{2-} , and one en molecule as ligand and two solvent water molecules. Each Zn^{2+} shows a tetragonal pyramid structure that coordinates to chelated N and O of a TTHQ^{2-} anion and a N(tetrazole) of another TTHQ^{2-} anionic ligand and an en molecule. The bond length of $\text{Zn}(1)-\text{O}(1)$ is 2.134(2) Å

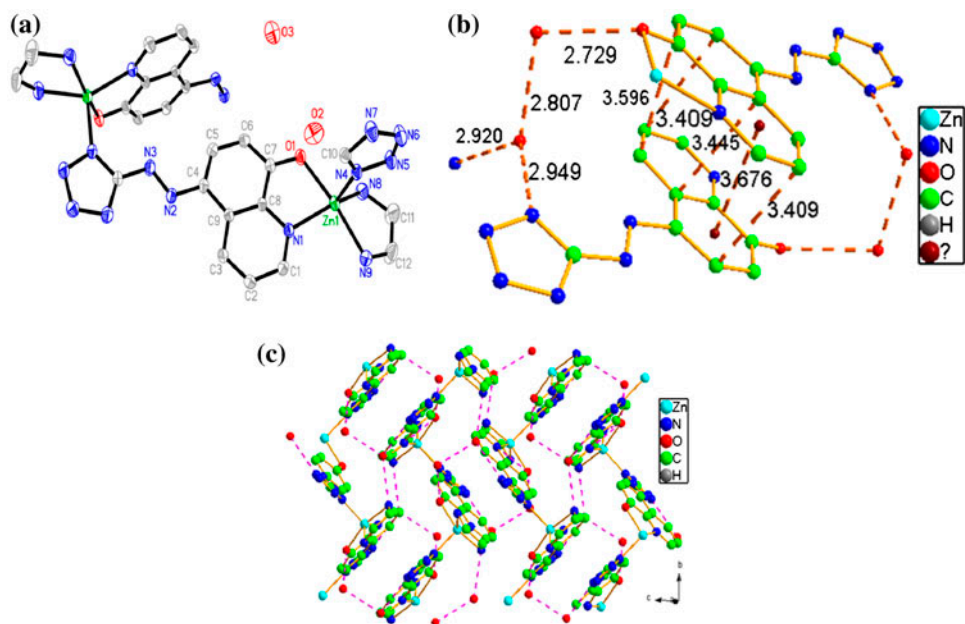


Figure 1. (a) The atom labeling diagram for **1**. (b) The diagram of π - π stacking interactions and hydrogen bonds in **1**. (c) The 2D supramolecular structure of **1**. All hydrogens and lattice water molecules have been omitted for clarity.

and the bond lengths of Zn(1)–N(1), Zn(1)–N(4), Zn(1)–N(8), and Zn(1)–N(9) are 2.0741(24), 2.0355(25), 2.0638(30), and 2.1447(27) Å, respectively. Each coordinating TTHQ²⁻ links to two different Zn²⁺ ions to give a 1-D zigzag chain structure. In **1**, the TTHQ²⁻ exhibits a *trans*-enol isomer with C–O bond length of 1.2860(34) Å and the tetrazole ring and hydroxyquinoline ring are almost coplanar with dihedral angle of 13.34°. A slipped face-to-face π – π stacking interaction was observed between two quinoline rings with the interplanar shortest atom-to-atom distance of 3.409 Å and interplanar center-to-center distance of 3.676 Å [figure 1(b)]. Three kinds of hydrogen bonds of two O–H \cdots O and a O–H \cdots N are observed between solvent water molecules with O \cdots O distance of 2.807 Å, between phenolic oxygen and solvent water with O \cdots O distance of 2.729 Å and between solvent water and tetrazole moiety with O \cdots N distance of 2.949 Å. These hydrogen bonds together with π – π stacking interactions link the complex moieties and lattice water molecules to form a 2D supramolecular structure [figure 1(c)].

3.1.2. The crystal structure of [Mn₂(TTHQ)₂(H₂O)₆] \cdot 2H₂O (2**).** The atomic labeling diagram of **2** is shown in figure 2(a). Complex **2** crystallizes in the monoclinic space group *P2₁/c*. Each unit cell of **2** consists of two Mn²⁺ ions, two TTHQ²⁻ anions, six coordinated water molecules and two lattice water molecules. Each Mn²⁺ coordinates to chelated N and O of a TTHQ²⁻ and a N(tetrazole) of another TTHQ²⁻ ligand and three water molecules to give a distorted octahedral geometry with Mn(1)–N(1) and Mn(1)–N(7) bond lengths of 2.2446(15) and 2.2456(16) Å and Mn(1)–O(1), Mn(1)–O(2), Mn(1)–O(3), Mn(1)–O(4) bond lengths of 2.1499(14), 2.1528(15), 2.1757(16), 2.2015(15) Å and the axial O–Mn–N bond angle of 175.0°. Each coordinating TTHQ²⁻ links two different Mn²⁺ ions to give a

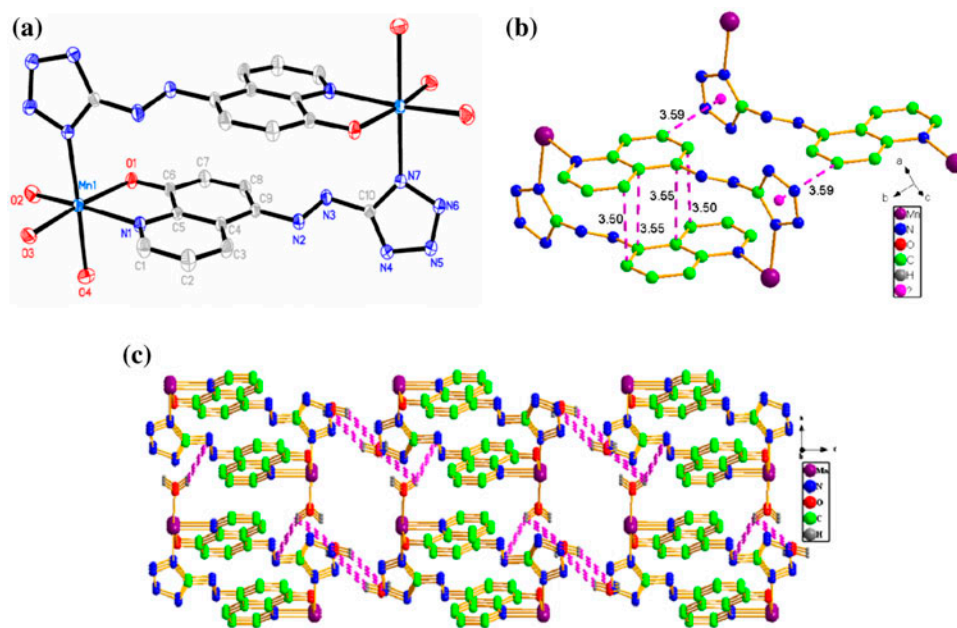


Figure 2. (a) The atom labeling diagram for **2**. (b) The diagram of π – π stacking interactions in **2**. (c) The 3D supramolecular structure of **2**. All hydrogens and lattice water molecules have been omitted for clarity.

binuclear structure. The TTHQ^{2-} anion also exhibits a *trans*-enol isomer with C–O bond length of 1.3057(21) Å and the tetrazole ring and hydroxyquinoline ring are nearly perpendicular with dihedral angle of 86.53°. The C–H $\cdots\pi$ between tetrazole and hydroxyquinoline ring with the distance of 3.59 Å and edge-to-edge π – π stacking interactions between two quinoline rings with the shortest atom-to-atom distance of 3.50 Å were observed [figure 2(b)]. Three kinds of hydrogen bonds of one O–H \cdots O and two O–H \cdots N are observed between coordinated and lattice water molecules with O \cdots O shortest distance of 2.833 Å, between coordinated water and tetrazole nitrogen with O \cdots N distance of 2.764 Å and between coordinated water molecule and azo nitrogen with O \cdots N distance of 2.935 Å. These hydrogen bonds together with π – π stacking interactions link the complex moieties and lattice water molecules to form a 3-D supramolecular structure [figure 2(c)].

3.2. UV–vis spectral changes of TTHQ, **1** and **2**

The UV–vis spectra are often used to characterize the *trans*-*cis* isomerization of azo compounds. The TTHQ solution in DMF ($8 \times 10^{-5} \text{ mol dm}^{-3}$) undergoes *trans*-to-*cis* photoisomerization under irradiation of 365 nm UV light. As shown in figure 3(a), the absorption intensity of the π – π^* transition around 380 nm decreases, while the absorption intensity of n – π^* transition around 465 nm slightly increases. The existence of isobestic points at 285 and 430 nm is characteristic for the presence of two distinct absorbing species in equilibrium with each other and demonstrates that no side reaction took place during the photoisomerization process [31]. Figure 3(b) gives the UV–vis spectral changes under 365 nm UV irradiation of **1** in DMF ($8 \times 10^{-5} \text{ mol dm}^{-3}$). **1** displays two absorption bands at 393 and 507 nm and the two absorptions decrease upon photoirradiation. **2** displays one absorption at 444 nm and the peak increases upon photoirradiation [figure 3(c)]. The absorption bands for TTHQ, **1** and **2** should originate from the π electronic transitions of TTHQ [32]. Moreover, the UV–vis spectral changes of TTHQ, **1** and **2** in DMF are in accord with the first-order kinetics (Supplementary Material, figure S2), and the rate constants are 4.092×10^{-2} , 5.336×10^{-2} and $3.793 \times 10^{-2} \text{ min}^{-1}$, respectively [33].

3.3. Photoluminescence for the solution of TTHQ, **1** and **2**

The fluorescence spectra of TTHQ, **1** and **2** in DMF with concentration of $8 \times 10^{-5} \text{ mol dm}^{-3}$ are shown in figure 4. Insets are their excitation spectra. TTHQ displays a blue emission peak at 475 nm under 372 nm excitation [figure 4(a)]. **1** and **2** also exhibit blue emission peaks

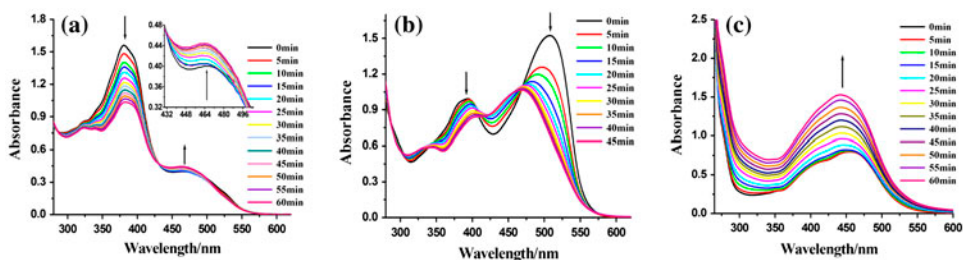


Figure 3. The UV–vis spectral changes under 365 nm UV light irradiation at 5-min intervals of TTHQ, **1** and **2** in DMF, respectively.

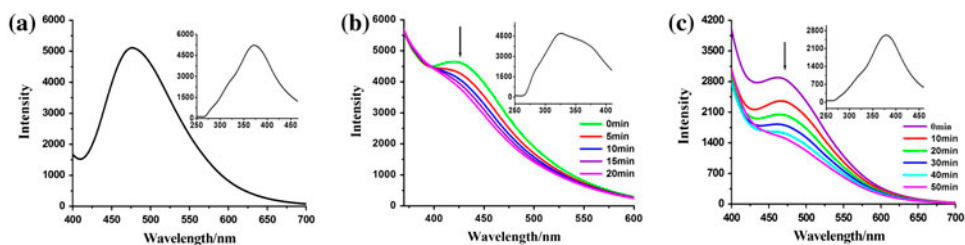


Figure 4. (a) The luminescence spectrum of TTHQ in DMF under 372 nm UV light excitation. (b) The luminescent spectrum of **1** in DMF under 326 nm UV light excitation. (c) The luminescent spectrum of **2** in DMF under 380 nm UV light excitation. Insets are the excitation spectra.

around 420 and 466 nm, respectively. The fluorescence intensity of **1** and **2** in DMF decreases dramatically upon UV light irradiation, while TTHQ does not show this property. As the irradiation time extends, **1** and **2** are almost nonfluorescent [figure 4(b) and (c)]. Generally, the H-aggregation of azo compounds could be destroyed under the irradiation of UV light [34]. Therefore, it is the broken aggregation that is responsible for the decrease of fluorescence intensity.

3.4. Solid photoluminescence of TTHQ and **1**

Photoluminescent properties for the solid samples of TTHQ and **1** are investigated at room temperature. Figure 5(a) shows the emission spectrum of TTHQ under 483 nm green–blue light excitation, and the inset shows the excitation spectrum with the monitored incident beam at 719 nm. TTHQ exhibits a red fluorescence band at 719 nm under 483 nm blue–green light excitation. The large Stokes shift of the fluorescent band for TTHQ may be attributed to the radiative relaxation of the excited *cis*-enol* of TTHQ that originates from a photoisomeric reaction under blue–green light excitation. The irradiation of Vis light of the *trans*-enol form leads to formation of the excited *trans*-enol* form. This species can complete a fast photoisomerization to the excited *cis*-enol* form. Figure 5(b) shows the emission spectrum of **1** under 490 nm blue–green light excitation, and the inset shows the

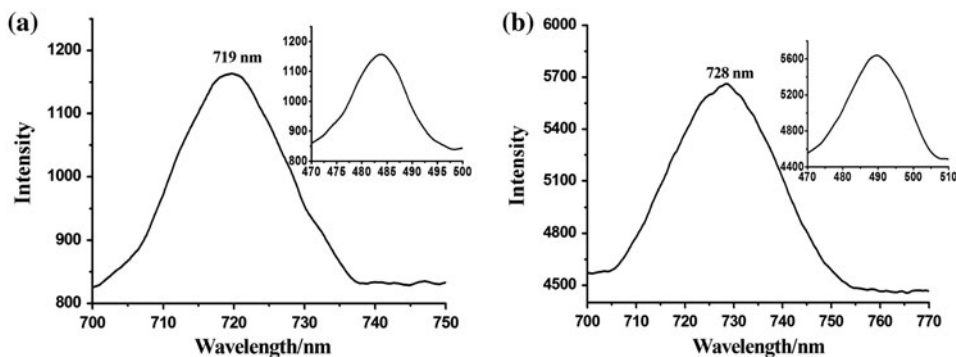


Figure 5. (a) The emission spectrum of solid TTHQ under 483 nm irradiation. (b) The emission spectrum of solid **1** under 490 nm irradiation. Insets are their excitation spectra.

excitation spectrum with the monitored incident beam at 728 nm. Complex **1** also exhibits a red fluorescence at 728 nm under 490 nm blue–green light excitation. Photoluminescence QY recorded at room temperature for solid samples of **1** is 13%.

3.5. Hydrogen-bonding interaction energies of **1** and **2**

To gain understanding of intermolecular hydrogen-bonding interactions for the solids of **1** and **2**, DFT was employed to obtain corresponding energies. The calculated energies are based on the crystal structures obtained in this work. The calculated hydrogen-bonding interaction energies of **1** and **2** are listed in table S1 (Supplementary Material). The hydrogen-bonding interaction energies with DFT/WB97XD method for **1** are 24.23–60.76 kJ mol⁻¹. The MP2 calculated hydrogen-bonding interaction energies for **1** are 20.23–49.28 kJ mol⁻¹. The DFT/WB97XD and MP2 calculated hydrogen-bonding interaction energies for **2** are 25.29–53.30 and 21.41–43.32 kJ mol⁻¹, respectively.

4. Conclusion

Two 5-tetrazolylazo-8-hydroxyquinoline (TTHQ) Zn²⁺ and Mn²⁺ complexes of **1** and **2** were synthesized, and the red photoluminescence of TTHQ and **1** was characterized and demonstrated. The photoluminescence promises a red photoluminescent material that may be applied to a full color display including light emitting diodes and other optoelectronic devices. Our results also provide a useful strategy to adjust structures and properties in the design of new photoluminescent functional coordination complexes based on 8-hydroxyquinoline derivatives as ligands.

Supplementary material

Crystallographic data have been deposited in the Cambridge Crystallographic Database Center. CCDC reference numbers are 975072 for **1** and 1036107 for **2**. These data can be obtained free of charge from the Cambridge Crystallographic Data Center via www.ccdc.cam.ac.uk/data_request/cif. The synthesis of TTHQ, the ¹H NMR spectrum of TTHQ, the first-order kinetics for the UV–vis spectral changes of TTHQ, **1** and **2**, the calculated hydrogen-bonding interaction energies of **1** and **2** are shown in Supplementary Material.

Disclosure statement

No potential conflict of interest was reported by the authors.

Funding

This work was supported by the National Natural Science Foundation of China [grant number 21271052]; Science and Technology Program Foundation of Guangzhou [grant number 2013J4100016]; Program Foundation of the Second Batch of Innovation Teams of Guangzhou Bureau of Education [grant number 13C04].

Supplemental data

Supplemental data for this article can be accessed at <http://dx.doi.org/10.1080/00958972.2015.1080824>.

References

- [1] C.W. Tang, S.A. Van Slyke. *Appl. Phys. Lett.*, **51**, 913 (1987).
- [2] M.A. Baldo, D.F. O'Brien, Y. You, A. Shoustikov, S. Sibley, M.E. Thompson, S.R. Forrest. *Nature*, **395**, 151 (1998).
- [3] V.P. Barberis, J.A. Mikroyannidis. *Synth. Met.*, **156**, 865 (2006).
- [4] A. Sharma, D. Singh, J.K. Makrandi, M.N. Kamalasanan, R. Shrivastva, I. Singh. *Mater. Lett.*, **61**, 4614 (2007).
- [5] G. Bandoli, A. Dolmella, F. Tisato, M. Porchia, F. Refosco. *Coord. Chem. Rev.*, **253**, 56 (2009).
- [6] M.J. Hannon. *Pure Appl. Chem.*, **79**, 2243 (2007).
- [7] A.R. Timerbaev. *Metallomics*, **1**, 193 (2009).
- [8] C. Deraeve, C. Boldron, A. Maraval, H. Mazarguil, H. Gornitzka, L. Vendier, M. Pitié, B. Meunier. *Chem. – Eur. J.*, **14**, 682 (2008).
- [9] M. Ghedini, M.L. Deda, I. Aiello, A. Grisolia. *Inorg. Chim. Acta*, **33**, 357 (2004).
- [10] M.M. El-Nahass, A.M. Farid, A.A. Atta. *J. Alloys Compd.*, **507**, 112 (2010).
- [11] R. Pohl, V.A. Montes, J. Shinar, P. Anzenbacher Jr. *J. Org. Chem.*, **69**, 1723 (2004).
- [12] S.-J. Li, Y. Li, J.-A. Zhang. *Inorg. Chem. Commun.*, **20**, 334 (2012).
- [13] E. Hao, T. Meng, M. Zhang, W.-D. Pang, Y.-Y. Zhou, L.-J. Jiao. *Phys. Chem. A*, **115**, 8234 (2011).
- [14] Y. Kang, C. Seward, D. Song, S. Wang. *Inorg. Chem.*, **42**, 2789 (2003).
- [15] M.A. Palacios, Z. Wang, V.A. Montes, G.V. Zyranov, P. Anzenbacher Jr. *J. Am. Chem. Soc.*, **130**, 10307 (2008).
- [16] M.A. Palacios, Z. Wang, V.A. Montes, G.V. Zyranov, B.J. Hausch, K. Jursikova, P. Anzenbacher Jr. *Chem. Commun.*, **36**, 3708 (2007).
- [17] V.M. Manninen, W.A.E. Omar, J.P. Heiskanen, H.J. Lemmetyinen, O.E.O. Hormi. *J. Mater. Chem.*, **22**, 22971 (2012).
- [18] Y.-K. Han, S.-U. Lee. *Chem. Phys. Lett.*, **366**, 9 (2002).
- [19] V.A. Montes, R. Pohl, J. Shinar, P. Anzenbacher Jr. *Chem. – Eur. J.*, **12**, 4523 (2006).
- [20] A.S. Kumar, T. Ye, T. Takami, B.C. Yu, A.K. Flatt, J.M. Tour, P.S. Weiss. *Nano Lett.*, **8**, 1644 (2008).
- [21] T. Sasaki, J.M. Tour. *Org. Lett.*, **10**, 897 (2008).
- [22] W.R. Browne, B.L. Feringa. *Annu. Rev. Phys. Chem.*, **60**, 407 (2009).
- [23] T.M. Klapötke, D.G. Piercey. *Inorg. Chem.*, **50**, 2732 (2011).
- [24] Y.-C. Li, C. Qi, S.-H. Li, H.-J. Zhang, C.-H. Sun, Y.-Z. Yu, S.-P. Pang. *J. Am. Chem. Soc.*, **132**, 12172 (2010).
- [25] P. Pratihar, T.K. Mondal, A.K. Patra, C. Sinha. *Inorg. Chem.*, **48**, 2760 (2009).
- [26] J.-M. Lin, W.-B. Chen, X.-M. Lin, A.-H. Lin, C.-Y. Ma, W. Dong, C.-E. Tian. *Chem. Commun.*, **47**, 2402 (2011).
- [27] G.M. Sheldrick. *SHELXS-97, Program for Solution of Crystal Structures*, University of Göttingen, Göttingen (1997).
- [28] G.M. Sheldrick. *SHELXL-97, Program for Refinement of Crystal Structures*, University of Göttingen, Göttingen (1997).
- [29] M.J. Frisch, G.W. Trucks, H.B. Schlegel, G.E. Scuseria, M.A. Robb, J.R. Cheeseman, G. Scalman, V. Barone, B. Mennucci, G.A. Petersson, H. Nakatsuji, M. Caricato, X. Li, H.P. Hratchian, A.F. Izmaylov, J. Bloino, G. Zheng, J.L. Sonnenberg, M. Hada, M. Ehara, K. Toyota, R. Fukuda, J. Hasegawa, M. Ishida, T. Nakajima, Y. Honda, O. Kitao, H. Nakai, T. Vreven, J.A. Montgomery, Jr., J.E. Peralta, F. Ogliaro, M. Bearpark, J.J. Heyd, E. Brothers, K.N. Kudin, V.N. Staroverov, R. Kobayashi, J. Normand, K. Raghavachari, A. Rendell, J.C. Burant, S.S. Iyengar, J. Tomasi, M. Cossi, N. Rega, J.M. Millam, M. Klene, J.E. Knox, J.B. Cross, V. Bakken, C. Adamo, J. Jaramillo, R. Gomperts, R.E. Stratmann, O. Yazyev, A.J. Austin, R. Cammi, C. Pomelli, J.W. Ochterski, R.L. Martin, K. Morokuma, V.G. Zakrzewski, G.A. Voth, P. Salvador, J.J. Dannenberg, S. Dapprich, A.D. Daniels, O. Farkas, J.B. Foresman, J.V. Ortiz, J. Cioslowski, D.J. Fox. *Gaussian 09, Revision A. 02*, Gaussian Inc., Wallingford, CT (2009).
- [30] S.F. Boys, F. Bernardi. *Mol. Phys.*, **19**, 553 (1970).
- [31] M. Niemann, H. Ritter. *Makromol. Chem.*, **194**, 1169 (1993).
- [32] G.-Z. Yuan, Y.-P. Huo, X.-L. Nie, X.-M. Fang, S.-Z. Zhu. *Tetrahedron*, **68**, 8018 (2012).
- [33] H. Ren, D. Chen, Y. Shi, H. Yu, Z. Fu. *Polym. Chem.*, **6**, 270 (2015).
- [34] Y. Wu, Y. Demachi, O. Tsutsumi, A. Kanazawa, T. Shiono, T. Ikeda. *Macromolecules*, **31**, 4457 (1998).